Journal of Vegetation Science 13: 817-830, 2002
© IAVS; Opulus Press Uppsala.

A model for seasonality and distribution of leaf area index of forests and its application to China

Luo, Tianxiang[1*]; Neilson, Ronald P.[2]; Tian, Hanqin[3]; Vörösmarty, Charles J.[4]; Zhu, Huazhong[1] & Liu, Shirong[5]

[1]*Institute of Geographical Sciences and Natural Resources Research, Chinese Academy of Sciences, P.O. Box 9717, Beijing 100101, China;*
[2]*USDA Forest Service, Oregon State University, Oregon 97333, USA;*
[3]*Department of Ecology and Evolutionary Biology, University of Kansas, KS 66045, USA;*
[4]*Institute for the Study of Earth, Oceans and Space, University of New Hampshire, Durham, NH 03824, USA;*
[5]*Institute of Forestry Ecology and Environment Protection, Chinese Academy of Forestry, Beijing 100091, China;*
Corresponding author; Fax: +861064889399; E-mail luotx@igsnrr.ac.cn, luotx@cern.ac.cn

Abstract. We have constructed a phenological model of leaf area index (*LAI*) of forests based on biological principles of leaf growth. Field data of maximum *LAI* from 794 plots with mature or nearly mature stand ages over China were used to parameterize and calibrate the model. New measurements of maximum *LAI* from 16 natural forest sites were used to validate the simulated maximum *LAI*. The predictions of seasonal *LAI* patterns were compared with seasonal changes derived from the 1-km satellite AVHRR-*NDVI* data for nine undisturbed forest sites in eastern China. Then, we used the model to map maximum *LAI* values for forests in China.

Model results indicated that the PhenLAI model generally predicted maximum *LAI* well for most forest types, even when maximum *LAI* is > 6. This suggests an ecological approach to the saturation problem in satellite detection of high forest *LAI* where the relationship between *NDVI* and *LAI* reaches an asymptote near a projected *LAI* value of 5 or 6. Furthermore, the predictions of seasonal *LAI* patterns in timing and dynamics were generally consistent with the satellite *NDVI* changes, except for monsoon forest and rain forest in south China where satellite detection of seasonal variation in leaf area is hardly possible. Compared with average projected *LAI* measurements of global forests from 809 field plots in literature data, our maximum *LAI* values were close to the global literature data for most of Chinese forests, but the average area-weighted maximum *LAI* for all forests of China (6.68 ± 3.85) was higher than the global mean *LAI* of the 809 field plots (5.55 ± 4.14). We believe that forest *LAI* in China is commonly > 6, especially in tropical rainforest, subtropical evergreen broad-leaved forest, temperate mixed forest, and boreal/alpine spruce-fir forest where satellite detection of high *LAI* is hardly possible.

Keywords: *LAI*; Leaf growth; Leaf mass; Modelling; *NDVI*; Phenology.

Abbreviations: *LAI* = Leaf Area Index; *NDVI* = Normalized Difference Vegetation Index; fPAR = Fraction of incoming Photosynthetically Active Radiation absorbed by plant canopy; WBM = Water balance model.

Introduction

Leaf area index (*LAI*) is defined as the assimilative leaf area relative to the projected ground area for a plant community (one-side area for broad-leaved trees and curve surface area exposed to sunlight for coniferous trees). In recent global change modelling, *LAI* has been widely used as an important variable in relation to carbon, water and energy fluxes (Woodward 1987; Running et al. 1989; Prentice et al. 1992; Neilson 1995). Much uncertainty in quantifying *LAI* exists due to the limitation of our understanding of biological processes that determine the magnitude and distribution of *LAI*.

Several approaches have been used to study the phenology of leaf mass and productivity, including: (1) length of the growing season, (2) life cycles and duration of phenophases, (3) growth analysis, (4) correlations between environmental factors and phenological events, (5) modelling and monitoring of seasonal carbon dynamics. Traditional techniques are based on phenological observations and climate data, e.g. 'phenometry' (Lieth 1970), 'heat-units' (Wang 1960), 'degree-days' (Thomson & Moncrieff 1982; Hunter & Lechowicz 1992) or 'chill-days' (Landsberg 1974; Cannell & Smith 1983; Murray et al. 1989). These techniques have been used for modelling development phases (phenophases) in plant life cycles (e.g. phenological spectrum) and quantitative changes within one phenophase. More advanced techniques for modelling onset and offset of greenness and seasonal carbon dynamics of regional/global vegetation include: (1) computer simulations of carbon flux by maximizing plant carbon gain (Janecek et al. 1989; Kikuzawa 1995; Woodward et al. 1995) or site water balance (Neilson 1995); (2) satellite monitoring based on the relation of *LAI* to *NDVI* (Normalized Difference Vegetation Index) (Spanner et al. 1990; Curran et al. 1992; White et al. 1997) or the relation of fPAR (the fraction of incoming photosynthetically active radiation absorbed by the canopy) to *NDVI* or other satellite vegetation index (Prince 1991a; Ruimy et al. 1994; Goetz & Prince 1996); (3) combinations of these first two approaches (e.g. Field et al. 1995; Hunt et al. 1996).

Measurements of *LAI* by satellite data (*NDVI* or fPAR) have been largely successful in croplands and grasslands (e.g. Prince 1991a; Daughtry et al. 1992), but some problems remain where *LAI* is high, such as forests where stand *LAI* is commonly > 6. These problems exist because the regression equations of *NDVI* or fPAR to *LAI* reach an asymptote around a projected *LAI* value of 5 or 6 (Sellers 1985; Spanner et al. 1990; Prince 1991b; Curran et al. 1992). Because of the saturation problem, satellite detection of seasonal variation in leaf area of southern evergreen forests is hardly possible (White et al. 1997). Considerable seasonality can exist in evergreen forests, but satellite observations of vegetation phenology almost always focus on deciduous forests or annual grasslands and croplands.

Although the most sophisticated models are based on simulations of ecosystem processes, they are not satisfactory for application at a global scale due to the lack of parameters for most of the world ecosystems (Ruimy et al. 1994). One of the critical gaps in developing a dynamic biosphere model is a poor understanding of how to scale up and the inability to validate such a model (Tian et al. 1998). *LAI* is the most important variable for measuring vegetation structure over large areas, and for relating it to energy and mass exchanges. In recent large-scale ecosystem modelling, *LAI* has been treated as an important variable. However, most of the published biogeography models and biogeochemistry models essentially consider *LAI* as an uncalibrated, internal state variable that is used to produce calibrated variables, such as vegetation carbon or vegetation types. The *LAI* outputs from various models differ greatly in magnitude and distribution (R.J. Drapek, R.P. Neilson & VEMAP Members pers. comm.).

In this study, we present a phenological model of leaf area index (here called PhenLAI, the 'Phenology of Leaf Area Index'), based on the morphological characteristics of leaf growth and development instead of physiological processes and biogeochemical cycles. The field data of maximum *LAI* ($LAI_{\max}$) from 794 plots with mature or nearly mature stand ages collected by Luo (1996) are used to parameterize and calibrate the model. New measurements of $LAI_{\max}$ for 13 natural forest sites in the Tibetan Alpine Vegetation Transects (TAVT) from 1999-2000, and three natural forest sites in eastern China from the Chinese literature (1998-2001) are used to validate the simulated $LAI_{\max}$. The predictions of seasonal *LAI* patterns in timing and dynamics instead of the *LAI* values were compared with seasonal changes of the 1-km satellite AVHRR-*NDVI* for the nine undisturbed forest sites with area of > 1 km^2 from eight nature reserve areas in E. China. Observed data of annual actual evapotranspiration by the catchment technique (CT) in some typical forests of E China were used to validate the estimated actual evapotranspiration in the PhenLAI model. Then, we use the model to map $LAI_{\max}$ of forests.

Leaf Area Index variations in PhenLAI

Predictions of *LAI* are based on three general temporal and spatial patterns over a range of forests: (1) *LAI* increases initially with forest age, then decreases slightly; (2) it generally has one seasonal peak; (3) it changes regionally with temperature and precipitation variables.

Growth of leaf mass with increasing stand age

There is evidence that leaf mass of a forest community reaches a more or less steady state early in succession (Grier & Running 1977). In general, for a young stand, *LAI* increases as stand age increases, and reaches a maximum in the nearly mature or mature stages. This maximum can be maintained if sufficient resources are available (Tadaki 1977; Waring & Schlesinger 1985). In many even-aged forests, competition among trees results in some mortality before *LAI* approaches a maximum, so that *LAI* actually peaks and then decreases slightly, maintaining a plateau until the trees die. Maximum sustained *LAI* is often 10-20% less than peak *LAI* (Waring & Schlesinger 1985).

Seasonal changes of leaf mass

Generally, boreal and temperate forests are seasonal where leafing patterns seem to be governed mainly by seasonally changing temperature and radiation. Warm-temperate forests are moderately seasonal. Tropical and subtropical forests have variable phenological patterns throughout the year but with a major pulse in the summer. Then, seasonality of leaf mass for a site can be quantitatively described as a function of time only (Fig. 1), such as the symmetrical sine curve (Waggoner 1974) or Gaussian distribution (Lieth 1970). In temperate forests, Kikuzawa (1983, 1984) found for deciduous tree and deciduous/evergreen shrub species in Japan three leafing patterns over a growing season: (1) flush type, (2) intermediate type, and (3) succeeding type. Most of the leaf survivorship curves look like an inverse U-shape or a bell shape. Taylor (1974), Larcher (1975), Sharik & Barnes (1976), and Bormann & Likens (1979) observed similar leafing patterns for deciduous trees. Lowman (1992) reported three main leafing patterns in the rain forests of New South Wales: (1) seasonal growth leaves flushed synchronously, (2) intermittent growth leaves flushed over several months, and (3) continuous growth leaves flushed throughout the year with a summer peak. In fact, these patterns for evergreen trees correspond to the types of Kikuzawa. Analogous types of leafing patterns were reported in the boreal forests of Alaska (Chapin & Tryon 1983) and the Mediterranean shrubs of southern California (Field & Mooney 1983; Gill & Mahall 1986).

Geographical distribution patterns of leaf area index

LAI is another valuable criterion of vegetation production (e.g. Webb et al. 1983; Waring & Schlesinger 1985). Geographically, it has been shown that LAI_{max} is well correlated with long-term climate variables. On water-limited sites, the vegetation *LAI* will reach a maximum while all available soil water is utilized (Woodward 1987). The assumption of LAI_{max} production within water balance constraints has been generally supported based on physiological studies and regional water balance analyses (Grier & Running 1977; Woodward 1987; Stephenson 1990). Some important biogeography models are based on this fundamental assumption under which the water-limited vegetation type and density are calculated (Neilson 1995). Our early study on pattern analysis of forest *LAI* in China further indicated that the LAI_{max} distribution patterns vary with different forest types, and are controlled by long-term climatic variables such as annual mean temperature, annual precipitation, warmth index and moisture index, singly or in combination (Luo et al. 1997).

Model description

The seasonality of leaf development is mainly controlled by temperature and sunlight, *LAI* and leaf biomass by precipitation and soil moisture. Soil water balance and biological constraints control the geographical patterns of forest *LAI*. The effect of these factors on *LAI* is studied through a spatially explicit model, PhenLAI (Fig. 2).

Because of the lack of spatial information on stand ages over a large region, this model was used to predict the *LAI* phenology of nearly-mature or mature stands, in which the leaf mass reaches a more or less steady state. The PhenLAI model uses monthly climate data and soil- and vegetation-specific parameters. An initial LAI_{max} is calculated using the regression equations that relate LAI_{max} to temperature and moisture indices (Table 1). Then, initial LAI_{max} values were adjusted downwards according to the balance of available soil water and plant transpiration in the growing season. Using the input data of climate, vegetation type, soil texture and elevation, the soil water associated with long-term climate was calculated by the water balance model (WBM) of Vörösmarty et al. (1989) that relies on techniques developed by Thornthwaite & Mather (1957). Soil water calculations are then fed into the plant transpiration module adapted from Neilson (1995), in which plant transpiration was related to *LAI* and soil water content. Minimum *LAI* (LAI_{min}) is simulated from the adjusted LAI_{max} based on either estimated actual evapotranspiration or leaf life span. Growing season length is calculated from monthly temperatures by the Coutagne equation (Wang 1960; Lieth 1970). Using the adjusted LAI_{max} and LAI_{min} and growing season length we calculate an initial monthly

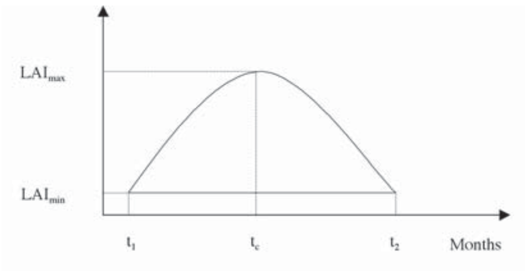

Fig. 1. The seasonal pattern of potential monthly *LAI*.

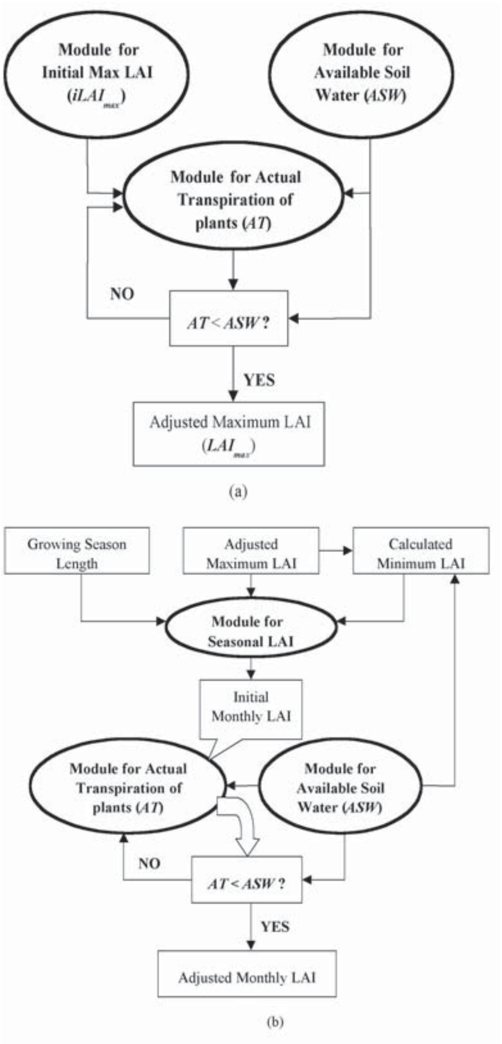

Fig. 2. A compartment flow diagram of the PhenLAI model.

LAI (LAI_{mo}) according to the Gaussian distribution. This initial LAI_{mo} is then adjusted downwards based on monthly soil water availability and plant transpiration.

All data sets used as inputs to drive the model are gridded at 2.5' latitude by 2.5' longitude (ca. 4-5 km), including climate (monthly mean temperature, precipitation, and cloudiness), vegetation type, soil texture and elevation. The data sets for monthly mean temperature and precipitation with elevation data were obtained from a Chinese 2.5' × 2.5' temperature and precipitation database (1960-1990) simulated by PRISM (Parameter-elevation Regressions on Independent Slopes Model; Daly et al. 1994, 2000). Cloudiness and soil texture data sets were derived from the 0.5° × 0.5° database of 30-yr mean monthly climatology (New et al. 2000), and from the 1° × 1° database of global soil texture (Webb et al. 2000). Data on forest types in China (Table 2) were according to the Vegetation Map of China by Hou (1979). The Phen*LAI* model was run monthly for each grid cell.

Initial LAI_{max} *module*

LAI_{max} in a mature stand reaches a more or less steady state that is associated with long-term climate (Grier & Running 1977; Woodward 1987; Stephenson 1990; Luo et al. 1997). In the module, the initial LAI_{max} were calculated from the regression equations between LAI_{max} and annual mean temperature and moisture indices for major forest types in China that were developed in our previous studies (Table 1). We developed the regressions according to the law of limiting factors (Odum 1971) in a geographical pattern that LAI_{max} decreased away from the optimum distribution centre of a forest type. These regressions were based on the field data for LAI_{max} from 794 plots with mature or nearly-mature stand ages that were selected from 668 ecological research plots in the Chinese literature before 1996 and 5175 inventory plots collected by Luo (1996). In this early study, we had collected 1285 biomass allometric regression equations for 98 tree species groups, and the ratios of specific leaf area (*SLA*) for 64 dominant tree species and undergrowth shrubs from the literature. Leaf biomass values of trees in the forest plots were estimated by the allometric regressions based on the measurements of tree height and DBH (diameter at breast height). Leaf biomasses of the undergrowth in the ecological research plots were measured by harvesting in quadrats (0.25 to 2 m^2), while those in the inventory plots were estimated based on the biomass ratios of undergrowth to trees that were collected from the literature. Then, we converted the leaf biomass densities of trees and shrubs to *LAI* values using the *SLA* ratios.

Available soil water module

To be comparable with the calculation of LAI_{max} of a mature stand based on long-term climate, the available soil water in a long-term balance state was calculated from the WBM of Vörösmarty et al. (1989). The WBM simulates a long-term water balance that relies on techniques developed by Thornthwaite & Mather (1957). Monthly soil water content as a percentage of total pore space (SWC_i,%) and available soil water (ASW_i, mm), monthly potential evapotranspiration (PET_i, mm) and estimated actual evapotranspiration (EET_i, mm) were obtained by running the WBM with the input data of vegetation type, climate (monthly mean temperature, precipitation and cloudiness), soil texture and elevation. The calculation of net irradiance was based on the input data of latitude and cloudiness. Field capacity and available water capacity of soil for each grid cell were determined as a function of vegetation class, soil texture and rooting depth. In the WBM, the estimates of plant rooting depth were based on the input data of vegetation type and soil texture. See further Vörösmarty et al. (1989).

Plant transpiration module

The above calculations of available soil water and potential evapotranspiration were fed into this module. In the module, actual transpiration (AT_i, mm) of plants was related to *LAI* and soil water content, in which plant transpiration increases as an exponential function of *LAI*

Table 1. Regression equations for distribution patterns of LAI_{max} in forests of China[1].

PhenLAI codes[2]	Regression equation	R^2	Plots	References
1, 3, 60, 62	$LAI = 1.70828 + 0.00029906 \cdot WI \cdot P$	0.7468	39	Luo (1996); Luo et al. (1997)
2, 6	$LAI = \exp(2.5062 - 0.0897 \cdot T)$	0.4996	136	Luo (1996); Luo et al. (1997)
4	$LAI = \exp(2.6722 - 0.14165 \cdot T)$	0.4041	126	Luo (1996); Luo et al. (1997)
5, 61, 64	$LAI = 8.0033 - 0.2103 \cdot (T - 18.5)^2$; $LAI = 3.0$ if $T < 14$ or $T > 24$	0.4076	58	Luo (1996); Luo et al. (1997)
63	$LAI = 8.228 - 0.2076 \cdot (\mathrm{T} - 16.6)^2$; $\mathrm{LAI} = 3.0$ if $T < 13$ or $T > 21$	0.5224	55	Luo (1996); Luo et al. (1997)
7, 8	$LAI = 5.616 \cdot \ln(MI) - 0.448 \cdot T$; $LAI = 0.6$ if $MI \leq 3.0$	0.9035	103	Luo (1996)
9, 10	$LAI = -4.62368 + 1.2582 \cdot MI$; $LAI = 1.0$ if $MI \leq 4.5$ and $MI \geq 3.0$; $LAI = 0.6$ if $MI \leq 3.0$	0.5601	93	Luo (1996)
12 to 18	$LAI = 1.2815 + 0.00034457 \cdot T \cdot P$	0.5439	184	Luo (1996)

[1] Significance level at $p < 0.001$. Variables and units in equations: *LAI*, leaf area index; T = annual mean temperature, °C; P = annual precipitation, mm; WI = Warmth index = sum of monthly mean temperature over 5°C in the year; MI = Moisture index $= P / (WI + 20)$ if $WI \leq 100$ or $2P / (WI + 140)$ if $WI > 100$ (Li 1985); ln = natural logarithm; exp = base of ln. [2] Forest type numbers explained in Table 2, col. 3.

Table 2. List of vegetation types with related leaf life span and leaf retention in average.

Forest types	Codes of Hou (1979)	Codes of PhenLAI	Leaf life span (yr)	Leaf retention (%)
Boreal coniferous deciduous forests dominated by *Larix gmelii*, *L. olgensis*, and *L. sibirica*	1, 2	1	< 1	0
Boreal spruce-fir evergreen forests on mountains in temperate zone	4, 5	2	5	80
Boreal spruce-fir evergreen forest on mountains in subtropical or tropical zones	15	6	5	80
Boreal evergreen pine forest dominated by *Pinus sylvestris* var. *Mongolica*	3	3	2	50
Boreal evergreen pine woodland on semi-arid sandy soil dominated by *Pinus sylvestris* var. *mongolica*	6	60	2	50
Temperate semi-arid evergreen pine forests dominated by *Pinus tabulaeformis*	7, 8	4	3	67
Temperate mixed forest of *Pinus koraiensis* and broad-leaved deciduous trees	16	7	4*	38
Subtropical evergreen pine forests on mountains dominated by *Pinus armandi*, *P. densata* etc.	10, 14	62	2	50
Subtropical evergreen coniferous woodland or plantation dominated by *Sabina* and *Cupressus*	13	64	3	67
Subtropical evergreen coniferous plantation dominated by Chinese-fir (*Cunninghamia lanceolata*)	12	63	2	50
Subtropical evergreen pine forest dominated by *Pinus yunnanensis* and *P. khasya*	11	5	1.5	33
Subtropical evergreen pine forest/plantation dominated by *Pinus massoniana*	9	61	1.5	33
Temperate typical deciduous broad-leaved forests	17, 18, 19	8	<1	0
Temperate deciduous microphyllous woodlands on semi-arid sandy soil or arid saline meadow soil	21, 22	10	<1	0
Temperate or subtropical deciduous microphyllous forest dominated by *Populus* and *Betula* species	20	9	<1	0
Subtropical evergreen-deciduous broad-leaved forests	23, 24, 25	12	2*	25
Subtropical evergreen broad-leaved forests	26, 27	13	2	50
Subtropical evergreen bamboo forest/plantation	30	16	2	50
Subtropical evergreen sclerophyllous forest dominated by *Quercus aquifolioides*	29	15	2	50
Subtropical monsoon evergreen broad-leaved forest	28	14	2	50
Tropical monsoon semi-evergreen broad-leaved forests	31, 32	17	2*	25
Tropical evergreen rainforest	33	18	2	50

* The percentage of evergreenness of the whole canopy is defined as 50%.

and stomatal conductance, and monthly potential evapotranspiration (PET_i) sets the upper limit of AT_i for each month (McMurtrie & Wolf 1983; Kunkel 1990; Saugier & Katerji 1991). Stomatal conductance was expressed as a function of soil water content and potential evapotranspiration (Neilson 1995). See further App. 1.

Seasonal LAI module

The seasonality of monthly potential *LAI* can be modelled with the following formula:

$$\mathrm{init}LAI_i = LAI_{\min} + (LAI_{\max} - LAI_{\min})\,(\exp(-k(t_i - t_c)^2)) \quad t_1 < t_i < t_2 \qquad (1)$$

$$\mathrm{init}LAI_i = LAI_{\min} \qquad k = (t_2 - t_1)^{-2} \qquad t_i \le t_1 \text{ or } t_i \ge t_2$$

$\mathrm{init}LAI_i$ is the initial LAI_{mo} ($-12 < i < 12$); t_c is the month during which $LAI_{\max}$ and actual evapotranspiration occur; t_1 is the month of leaf emergence; t_2 is the month of leaf fall; ($t_2 - t_1$) describes the length of the growing season (months) of the plants.

Determination of LAI$_{max}$

In a site with a given climate and specific forest type, the initial $LAI_{\max}$ was adjusted downwards based on the principle that actual transpiration of plants ($AT_{\max}$) should be less than the available soil water during the month t_c (ASW_i (t_c)). Moreover, the simulated $LAI_{\max}$ was constrained to fall below the maximum water use efficiency (*WUE*) that is the ratio of leaf area duration (*LAD*) to annual plant transpiration (ΣAT_i). The original definition of *WUE* is the ratio of the amount of carbon assimilated to the amount of water transpired (Eamus 1991). $LAI_{\max}$ is the accumulation of leaf growth during the growing season. According to Waring & Schlesinger (1985), gross primary production is related to leaf area duration, the product of $LAI_{\max}$ and ($t_2 - t_1$). The ratio of leaf area duration to annual plant transpiration can be considered as a surrogate for the maximum water use efficiency. For forests, *WUE* has been set to 0.25 (Neilson 1995).

Determination of LAI$_{min}$

$LAI_{\min}$ in deciduous forests was equal to 0. In evergreen forests, $LAI_{\min}$ was estimated from the adjusted $LAI_{\max}$ based on estimated evapotranspiration or leaf life span:

$$LAI_{\min} = LAI_{\max}(EET\,(t_1) + EET\,(t_2)) \,/\, (2 \cdot EET_{\max}) \quad \text{or}$$
$$LAI_{\min} = r \cdot LAI_{\max}, \text{ if } \; (EET\,(t_1) + EET\,(t_2)) \,/\, (2 \cdot EET_{\max}) < 0.25 \qquad (2)$$

$EET_{\max}$ is a maximum value of estimated monthly actual evapotranspiration, $EET\,(t_1)$ and $EET\,(t_2)$ are the estimated actual evapotranspiration in the months of t_2 and t_1, respectively, and *r* is the forest-type-specific value of leaf retention fraction from Table 2. For evergreen forests where the estimated actual evapotranspiration in the months t_2 and t_1 is very low or equal to 0, the $LAI_{\min}$ has a weak relationship to evapotranspiration. Then, we estimated $LAI_{\min}$ using a leaf-retention fraction based on its leaf life span.

Determination of growing season length

According to Coutagne's law of growth (Wang 1960; Lieth 1970), in a given climate, the optimum plant growth rate (*g*) is related to plant temperature (*x*) in a logistic function as follows:

$$g = a[exp(-((x - c) / n)^2)] \qquad (3)$$

where a is the coefficient of development rate ($1/a$ = longevity or growing time), c is the temperature for which the most rapid development of the plant is obtained, and n is the coefficient which describes the sensitivity of the plant to temperature (Wang 1960; Lieth 1970). Integration of this equation yields the total growing time of the plant at any given temperature, x (Lieth 1970). We set g as 1 or 100% for the whole growth during a year. Then, the reciprocal of a value defines the growing season length of a plant while c and n determine the temperature range of plant acclimatization. In the PhenLAI model, the growing season was calculated from the monthly temperature data by the following formula:

$$t_2 - t_1 = 1/a = \sum\left[\exp\left(-\left((x-c)/n\right)^2\right)\right] \quad x > 0°\mathrm{C} \qquad (4)$$

Here, x was defined as monthly mean temperature (°C) from the input climate data set, c equals 20 °C for the optimum temperature of photosynthesis, 0 °C is for the base temperature of leaf emergence, n equals the temperature range suitable for plant growth between 0 °C and 30 °C (Wang 1960; Anderson 1974).

In Eq. (1), t_c is defined as the month with $EET_{\max}$; t_1 and t_2 follow from

$t_1 = t_c - 1/(2 \cdot a)$

$t_2 = t_c + 1/(2 \cdot a)$ (5)

Determination of LAI_{mo}

Once $LAI_{\max}$, $LAI_{\min}$ and growing season length are defined, init*LAI* is calculated with Eq. (1); init*LAI* is then adjusted downwards based on monthly soil water availability and plant transpiration. If the winter climate is so cold that potential evapotranspiration approaches 0, we define LAI_i as $LAI_{\min}$. See further App. 1.

Site data for model validation

We used three kinds of site data over a range of forests to validate the model. 1. New measurements of $LAI_{\max}$ for the 13 natural forest sites from our recent study in the TAVT and the three natural forest sites in eastern China from Liu et al. (1998); Zheng et al. (2000) and Tsutsumi et al. (2001) (Table 3) were used to validate the simulated $LAI_{\max}$. 2. Seasonal changes of the 1-km AVHRR-*NDVI* for the nine undisturbed forest sites > 1 km^2 in eastern China (Table 4) were compared with the predictions of seasonal *LAI* patterns in timing and dynamics. 3. Observed data of annual actual evapotranspiration by the catchment technique (CT) in seven typical forests from five long-term research stations of eastern China were used to validate the estimated actual evapotranspiration (*EET*) in the Phen*LAI* model.

LAI_{max} measurements in the TAVT forest sites

The TAVT included an altitudinal transect in the east slope of Gongga Mountains (the peak is over 7000 m) of western Sichuan Province and a longitudinal-latitudinal transect on the Tibetan Plateau. The altitudinal transect started from subtropical evergreen broad-leaved forest at 1900 m to timberline at 3700 m. The longitudinal-latitudinal transect covered 29° 32' -35° 13' N and 91° 08'-94°43' E, ca. 1000 km long and 40 km wide. During July to September in 1999 and 2000, we measured live biomass density of trees and undergrowth in both below-ground and above-ground for 13 natural forest sites ranging from subtropical forest to alpine timberline forest or woodland (App. 2).

In each forest plot, tree height and DBH were measured for all trees of over 3 cm in DBH. Leaf biomass density of trees in the 13 forest plots were estimated by allometric regressions (App. 4) based on the measurements of tree height and DBH, while those of the undergrowth were measured by harvesting in a 2 m × 2 m quadrat. Moreover, we measured specific leaf area (SLA) of dominant tree species and undergrowth shrubs in different leaf age groups. Then, we converted the leaf biomass densities of trees and shrubs to *LAI* values using the biomass-weighted ratios of *SLA* in the 13 forest plots (Table 3, sites 1-13). For undergrowth herbs and lichens, the *LAI* estimates were based on the cover degrees because of difficulty in measurements of their *SLA* ratios.

To run the PhenLAI model at plot sites, we also measured the profile soil textures for the TAVT forest sites. Because of few meteorological observatories on the Tibetan Plateau, the climatic data of the sites along the longitudinal-latitudinal transect were obtained from the 2.5' × 2.5' Chinese temperature and precipitation database simulated by the PRISM model according to GPS locations (latitude, longitude and altitude). The climatic data of the sites along the altitudinal transect were estimated from the 10-yr meteorological observations measured at 1600 m and 3000 m, respectively, by the Alpine Ecosystem Observation and Experiment Station, Chinese Academy of Sciences. We calculated the site temperatures using a lapse rate of 0.6 °C per 100 m of altitude. Annual precipitation at elevation below 2500 m was estimated from the meteorological observatory at 1600 m in increments of 120 mm per 100 m. Annual precipitation at elevation above 2500 m was estimated from the meteorological observatory at 3000 m in decrements (between 2500 m and 3000 m) or increments (above 3000 m) of 74 mm per 100 m.

Table 3. Field data of maximum LAI_{max} in 16 undisturbed forest sites used for modeling validation. Sites 1 to 13 are from our recent study in the Tibetan Alpine Vegetation Transects (TAVT) during 1999-2000. Sites 14, 15 and 16 are from Liu et al. (1998), Tsutsumi et al. (2001) and Zheng et al. (2000), respectively, using the same methods to measure biomass and *LAI*.

Site	Place name	Vegetation type	Long.	Lat.	Alt. (m)	LAI_{max} trees	LAI_{max} undergrowth
1	East Mila Mt.	*Betula* deciduous forest	93º 30' 00"	30º 00' 00"	3620	5.59	0.10
2	Nyiyang River Valley	*Quercus* evergreen forest	94 01 19	29 45 35	3080	6.81	-
3	Nyiyang River Valley	Mixed forest of *Pinus densata* and *Quercus* evergreen trees	94 14 32	29 45 13	3080	5.91	0.80
4	West Sergyemla Mt.	Alpine fir forest of *Abies georgei* var. *smithii*	94 33 27	29 33 32	3780	11.41	1.00
5	West Sergyemla Mt.	Timberline forest of *Abies georgei* var. *smithii*	94 35 31	29 34 52	4073	7.86	1.00
6	West Sergyemla Mt.	Timberline woodland of *Sabina saltuaria and Rhododendron*	94 37 22	29 36 55	4450	4.54	-
7	East Sergyemla Mt.	Alpine fir forest of *Abies georgei* var. *smithii*	94 42 51	29 39 04	3800	9.18	1.00
8	East Gongga Mt.	Evergreen broad-leaved forest	102 03 26	29 36 16	1900	4.17	0.38
9	East Gongga Mt.	Evergreen-deciduous broad-leaved forest	102 01 28	29 35 13	2200	5.88	0.44
10	East Gongga Mt.	Mixed forest of spruce-fir and deciduous broad-leaved forest	102 01 20	29 35 10	2850	8.51	1.80
11	East Gongga Mt.	Alpine fir forest of *Abies fabri*	101 59 55	29 34 34	3050	6.68	1.10
12	East Gongga Mt.	Alpine fir forest of *Abies fabri*	101 59 55	29 34 34	3000	7.54	2.63
13	East Gongga Mt.	Timberline forest of *Abies fabri*	101 58 05	29 32 44	3700	7.72	2.49
14	Baotianman Reserve	*Quercus* deciduous forest	111 56 00	33 29 00	600	4.21	0.10
15	Jiulian Mt.	Evergreen broad-leaved forest	114 28 00	24 32 00	875	10.97	0.85
16	Xishuangbanna Reserve	Tropical monsoon rainforest	101 12 00	21 58 00	650	6.91	0.20

The 1-km AVHRR-NDVI data

Since field measurements of monthly *LAI* in forests are hardly possible, we have no field data to validate the simulated monthly *LAI* values. However, satellite AVHRR-*NDVI* time-series data can be used for observations of vegetation phenology such as greenness onset and offset, length of growing season, seasonal changes in vegetation coverage and evergreen/deciduous ratio that are to some extent related to *LAI* changes, especially in deciduous forests (Spanner et al. 1990; White et al. 1997). Considering the saturation problem in satellite detection of high forest *LAI* noted above, we used the 1-km *NDVI* time-series data to test the predictions of seasonal *LAI* patterns in timing and dynamics instead of the *LAI* values.

Considering serious influences of cloud and snow on the *NDVI* values as well as land-use and scale issues, we selected the nine forest sites in eastern China where there are undisturbed vegetation types with area of larger than l km^2, better *NDVI* data to reflect vegetation growth, and field measurements of maximum *LAI* available from the literature (Table 4). The 1-km *NDVI* 10-day composite data during February of 1995 to January of 1996 for the nine forest sites were obtained from the USGS EROS Data Center according to their latitudes and longitudes. The maximum monthly *NDVI* values were used in this study.

The seasonal *NDVI* changes were compared with the predictions of seasonal *LAI* patterns for the nine natural forest sites. Because of the lack of detail information on climate and soil from the literature, the climate and soil data sets used as inputs to drive the model were obtained from the Chinese 2.5' latitude by 2.5' longitude data sets described above.

Observations of actual evapotranspiration by the catchment technique

Observations of actual evapotranspiration in Chinese forests are still sparse. The observed data of annual actual evapotranspiration by the CT method in 7 typical forests from five long-term research stations of eastern China were obtained from Liu et al. (1996) and Li et al. (2001). The CT method for observing annual actual evapotranspiration is based on the law of conservation of mass: annual precipitation equals the sum of evapotranspiration, run-off and changes in soil water storage (SW), plant water content (PW) and litter water content (LW). For a long-term period such as one water year, the changes in SW, PW and LW approach zero. Then, annual actual evapotranspiration equals annual precipitation minus annual run-off.

Results

Comparison of predicted LAI_{max} with field data

The predicted LAI_{max} was significantly related to the field data from the 16 natural forest sites (Fig. 3; Table 3) ($R^2 = 0.5617$; $P < 0.001$) except for two forest sites in a dry river valley with below-ground water that was not included in our water balance model. Field LAI_{max} ranged from 4.31 in temperate deciduous forest to 12.41 in alpine fir forest, while predictions ranged from 2.6 in dry valley *Quercus* evergreen forest to 12.5 in subtropical evergreen broad-leaved forest (Fig. 3). Model accuracy was > 70% in 11 of the 16 plots. This suggested that the PhenLAI model generally predicted LAI_{max} well for most of forest types in China.

Table 4. Field maximum LAI and satellite maximum *NDVI* in nine undisturbed forest sites > 1 km^2 in eastern China. There is no relation between *LAI* and *NDVI*, because of the saturation problem in satellite detection of high forest *LAI*. The field LAI_{max} values include measurements of trees and undergrowth that are available from the literature. The 1-km satellite *NDVI* data are obtained from the USGS EROS Data Center. To compare *NDVI* with *LAI* in a graph, we multiply *NDVI* by 10 with a range from – 10 to 10. (see also App. 3.)

Place name	Vegetation type	Longitude	Latitude	LAI_{max}	$NDVI_{max}$	Reference
Changbai Mt. Reserve	Temperate mixed forest of pine and deciduous trees	E128 05 43	N42 24 05	10.20	8.6	Xu et al. (1985)
Changbai Mt. Reserve	Temperate mountain spruce-fir forest	E128 07 55	N42 08 37	15.37	7.8	Li et al. (1981)
Dongling Mt. Park	Temperate *Quercus* deciduous forest	E115 26 00	N40 00 00	11.43	8.0	Jiang (1997)
Baotianman Reserve	Temperate *Quercus* deciduous forest	E111 56 00	N33 29 00	4.31	7.1	Liu et al. (1998)
Jiulian Mt. Reserve	Subtropical evergreen broad-leaved forest	E114 28 00	N24 32 00	11.82	7.8	Tsutsumi et al. (2001)
Ailao Mt. Reserve	Subtropical mountain evergreen broad-leaved forest	E101 01 00	N24 32 00	9.50	7.4	Qiu & Xie (1998)
Dinghushan Reserve	Subtropical monsoon evergreen broad-leaved forest	E112 35 00	N23 10 00	17.76	8.1	Ren & Peng (1997)
Xishuangbanna Reserve	Tropical monsoon rainforest	E101 12 00	N21 58 00	7.11	7.6	Zheng et al. (2000)
Jianfengling Mt. Reserve	Tropical mountain rainforest	E108 55 00	N18 44 00	16.70	8.4	Li et al. (1996)

Seasonal LAI patterns and NDVI changes

In Fig. 4, seasonal *LAI* patterns simulated by the PhenLAI model are compared with the monthly *NDVI* changes in the nine undisturbed forest sites > 1 km^2 (Table 4). In general, predictions of seasonal *LAI* patterns were consistent with *NDVI* changes except monsoon forest and rain forest in S China. *LAI* and *NDVI* in temperate forests were seasonal since most of the trees shed their leaves in winter, get new leaves in spring and flourish in summer (Fig. 4 a-d). Tropical and subtropical forests had variable seasonal patterns of *LAI* and *NDVI* but with a major pulse in summer (Fig. 4e-i). In the Ailao Mts. (Fig. 4f), the predictions of seasonal *LAI* changes were consistent with observations of dominant tree species by Xie et al. (1997): leaf expansion starts in late March, is maximal in April to May and ends in June, leaf fall occurs in spring (from March to May) and winter (from November to December).

Comparison of estimated actual evapotranspiration with the field observation

Annual *EET* values in the PhenLAI model were significantly related to field observations by the CT method in seven typical forests of E China (Fig. 5) ($R^2 = 0.9668$, $P < 0.001$). *EET* was 1% to 16% higher than measurements by the CT method, indicating that the WBM of Vörösmarty et al. (1989) linked to the PhenLAI model is applicable to Chinese forests.

LAI_{max} in forests simulated by the PhenLAI model

The validated PhenLAI model was used to map LAI_{max} of forests in China (Fig. 7). The geographical distribution pattern of LAI_{max} showed a decreasing trend from SE to NW. At large scales, the area-weighted LAI_{max} varied from 2.43 to 8.77 in boreal forests, 1.89 to 10.13 in temperate forests, 2.97 to 10.49 in subtropical evergreen forests and 5.64 to 18.05 in tropical forests (Table 5). The *LAI* values for the tropical monsoon semi-evergreen broad-leaved forest and temperate deciduous microphyllous broad-leaved forest/woodland were most variable where coefficients of variation in maximum *LAI* were more than 95%, as contrasted with the temperate mixed forest and boreal *Larix* deciduous forest where coefficients of variation in maximum *LAI* were less than 43% (Table 5). The average area-weighted maximum *LAI* for all forests of China was 6.68 ± 3.85.

Discussion

Comparison of LAI_{max} estimates of Chinese forests with mean projected measurements of global forests

Mean *LAI* measurements of global forests were obtained from 809 field plots from literature data during 1932-2000 collected by Scurlock et al. (2001) (Table 6). The data were regrouped into comparable vegetation types with the Phen*LAI* forests based on similar dominant tree-species and climatic zones. The global field *LAI* varied by over an order of magnitude across biomes:

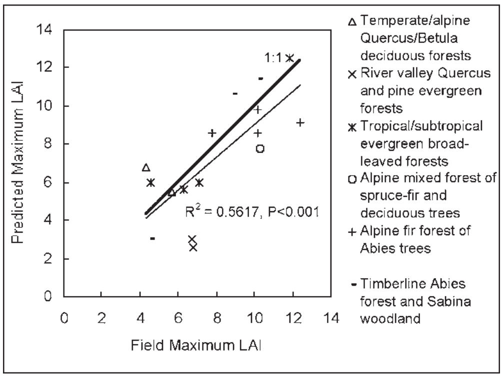

Fig. 3. Linear relationship between field LAI_{max} of 16 undisturbed forest sites (Table 3) and their predictions of LAI_{max} by the PhenLAI model.

Table 5. Estimates of LAI_{max} in forests of China by the PhenLAI model.

Forest type (PhenLAI codes)	Area-weighted LAI_{max}	Standard error	Coefficient of variation (%)
Boreal *Larix* deciduous forest (1)	6.15	2.66	43.32
Boreal/alpine *Picea-Abies* forest (2, 6)	8.77	4.78	54.43
Boreal/temperate *Pinus* forest/woodland (3-4, 60)	2.43	1.62	66.66
Temperate mixed forest of *Pinus* and deciduous trees (7)	10.13	3.93	38.79
Temperate typical deciduous broad-leaved forest (8)	6.00	4.58	76.44
Temperate deciduous microphyllous forest/woodland (9-10)	1.89	1.79	94.55
Subtropical evergreen coniferous forest/plantation (5, 61-64)	4.98	2.85	57.21
Subtropical evergreen broad-leaved forest (12-14, 16)	10.49	5.59	53.31
Subtropical evergreen sclerophyllous broad-leaved forest (15)	2.97	1.64	55.10
Tropical monsoon semi-evergreen broad-leaved forest (17)	5.64	5.59	99.17
Tropical evergreen rain forest (18)	18.05	11.74	65.06

Temperate evergreen broad-leaved forest in Japan: 8.70;
Boreal/temperate *Picea-Abies* and *Pseudotsuga-Abies* forests: 7.28;
Tropical evergreen broad-leaved forest: 6.29;
Temperate *Pinus* forest: 5.43;
Temperate deciduous broad-leaved forest: 5.41;
Boreal *Larix* deciduous forest: 4.63;
Temperate evergreen sclerophyllous broad-leaved forest: 4.23
Tropical deciduous broad-leaved forest: 3.92;
Boreal/temperate *Populus*/*Betula* forest/woodland: 2.84;
Boreal *Pinus* forest/woodland: 2.77.

Our simulated maximum *LAI* values were close to the literature data for most of Chinese forests such as boreal/temperate/alpine *Picea-Abies* forest (8.77 vs. 7.28) and *Pinus* woodland (2.43 vs. 2.77), temperate deciduous broad-leaved forest (6.00 vs. 5.41) and microphyllous forest/woodland (1.89 vs. 2.84), subtropical evergreen coniferous forest/plantation (4.98 vs. 5.43) and broad-leaved forest (10.49 vs. 8.70) (from Table 6). For other forest types, there were higher maximum *LAI* simulations in tropical evergreen rainforest (18.05 vs. 6.29), tropical monsoon semi-evergreen broad-leaved forest (5.64 vs. 3.92) and boreal *Larix* deciduous forest (6.15 vs. 4.63), while the predicted maximum *LAI* was lower in subtropical evergreen sclerophyllous broad-leaved forest (2.97 vs. 4.23). The average area-weighted maximum *LAI* for all forests of China (6.68 ± 3.85) was higher than the global average literature *LAI* of the 809 field plots (5.55 ± 4.14). In China, the tropical rain and monsoon forests reach their extreme northern limit in the world. We believe that the higher LAI_{max} in Chinese monsoon and rain forests is due to the relative cool and moist climate where the highest LAI_{max} (ca. 18) occurred (Tables 3 and 4). This comparison indicates that our predicted maximum *LAI* ranges at regional scales are acceptable.

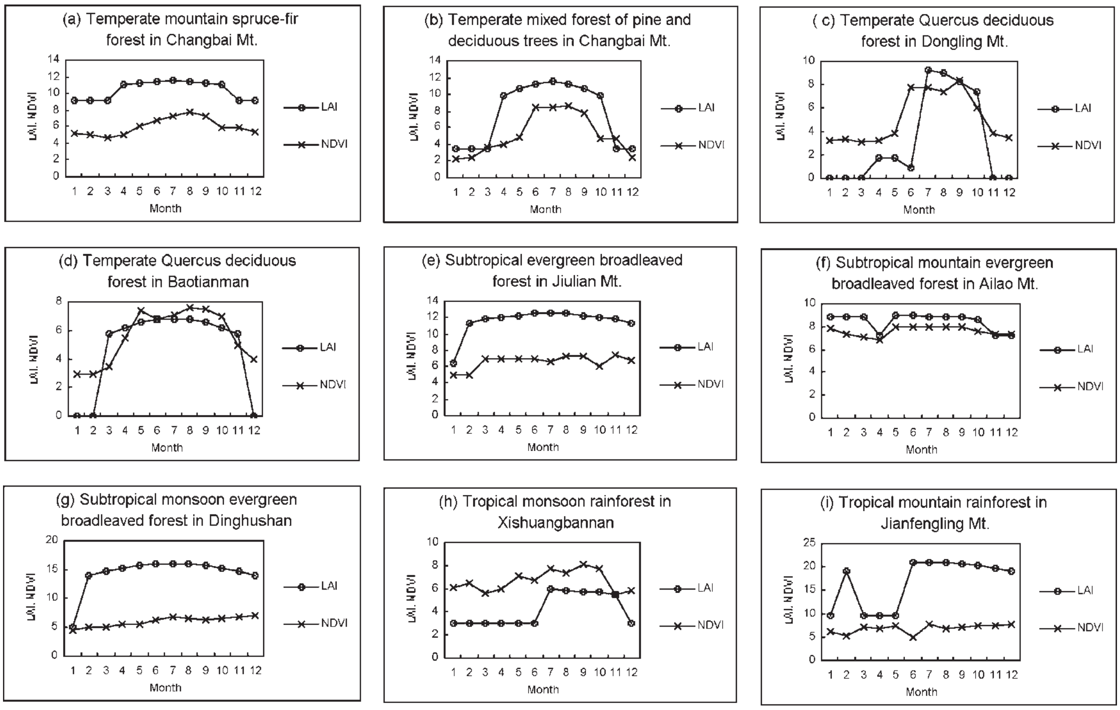

Fig. 4. Comparisons of simulated seasonal *LAI* patterns with seasonal *NDVI* changes for nine undisturbed forest sites (Table 4).

Table 6. Mean projected *LAI* measurements of forests from 809 field plots from world literature data from 1932-2000 (Scurlock et al. 2001) compared with model results in comparable vegetation types. Field data of forest *LAI* were measured by different methods. Because of limited information on stand age for most of the field plots, the mean *LAI* values were obtained directly from the literature data without consideration of stand age influences.

Forest types (comparable PhenLAI vegetation codes)	Average field LAI	Standard error	Field plots
Boreal *Larix* deciduous forest (1)	4.63 (6.15*)	2.37(2.66*)	17
Boreal/temperate *Picea-Abies* and *Pseudotsuga-Abies* forest (2, 6)	7.28 (8.77*)	6.79(4.78*)	126
Boreal *Pinus* forest/woodland (3-4, 60)	2.77 (2.43*)	2.19(1.62*)	25
Boreal/temperate *Populus*/*Betula* forest/woodland (9-10)	2.84 (1.89*)	1.21(1.79*)	84
Temperate *Pinus* forest (5, 61-64)	5.43 (4.98*)	4.18(2.85*)	200
Temperate typical deciduous broad-leaved forest (8)	5.41 (6.00*)	2.24(4.58*)	182
Temperate evergreen broad-leaved forest in Japan (12-14, 16)	8.70 (10.49*)	3.00(5.59*)	40
Temperate evergreen sclerophyllous broad-leaved forest (15)	4.23 (2.97*)	1.95(1.64*)	33
Tropical deciduous broad-leaved forest (17)	3.92 (5.64*)	2.53(5.59*)	18
Tropical evergreen broad-leaved forest (18)	6.29 (18.05*)	3.46(11.74*)	84

* Mean LAI_{max} of Chinese forests simulated by the PhenLAI model (Table 5).

Saturation problem in the detection of high forest LAI

In Fig. 6, field LAI_{max} values from 22 undisturbed forest sites > 1 km^2 (Tables 3 and 4) were related to satellite $NDVI_{max}$. Linear and curvilinear relationships (both with low correlation coefficients) indicated that the changes of $NDVI_{max}$, ranging from 6-9, were unable to explain large variations in field LAI_{max} (range 4-18). The relationship between simulated monthly *LAI* and satellite monthly *NDVI* (Table 4) showed a similar trend (Fig. 8). The saturation problem, following from the fact that the regression equations of *NDVI* to *LAI* reach an asymptote, has recently been noticed (Cihlar et al. 2000).

Fig. 3 indicates that the PhenLAI model generally predicted LAI_{max} well for most of forest types in China even when the maximum *LAI* is greater than 6, suggesting an ecological approach to the saturation problem in satellite detection of high forest *LAI*. Furthermore, the predictions of seasonal *LAI* patterns in timing and dynamics were generally consistent with the satellite *NDVI* changes except monsoon forest and rainforest in south China (Fig. 4), indirectly indicating that the simulations of monthly *LAI* were well based. White et al. (1997) suggested that although considerable seasonality can exist in evergreen forests, satellite detection of seasonal variation in leaf area of southern evergreen forests is hardly possible.

Explanations for high LAI measurements in forests

High measurements of forest *LAI* have been questioned in methodology since Marshall & Waring (1986) reported that estimates of leaf area based on tree diameter appear to be inaccurate and therefore the exceedingly high leaf-area indices previously reported for Douglas-fir forests are unreliable. However, Ren & Peng (1997) presented a research result different from Marshall & Waring (1986) based on their study on comparisons

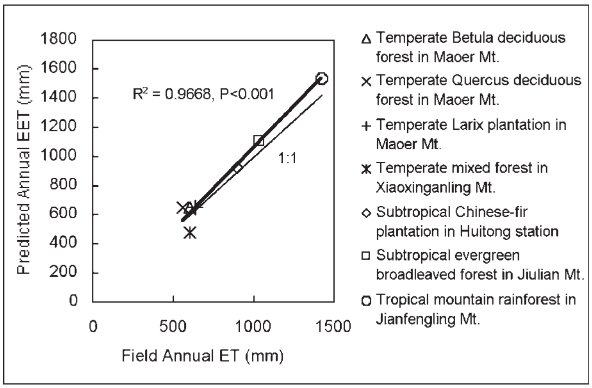

Fig. 5. Linear relationship between observations of annual actual evapotranspiration (*ET*) by the catchment technique and estimated actual evapotranspiration (*EET*) in the PhenLAI model. Field data are the means of 2-6 yr observations in seven typical forests in E China (Liu et al. 1996; Li et al. 2001).

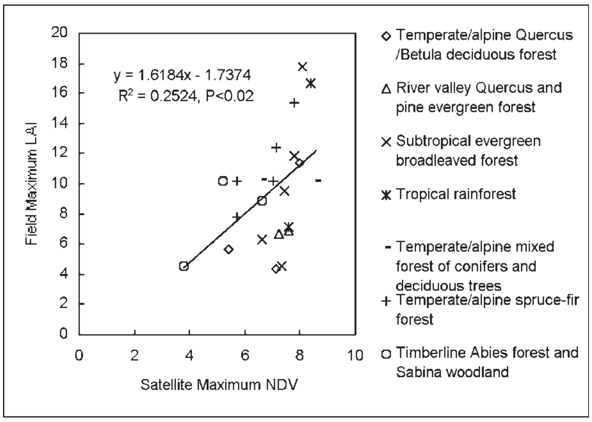

Fig. 6. Relationship between satellite maximum *NDVI* and field maximum *LAI* from the 22 undisturbed forest sites in Tables 3 and 4. The *LAI-NDVI* comparison clearly demonstrates the lack of a relation between *LAI* and *NDVI*, because of the saturation problem in satellite detection of high forest *LAI*.

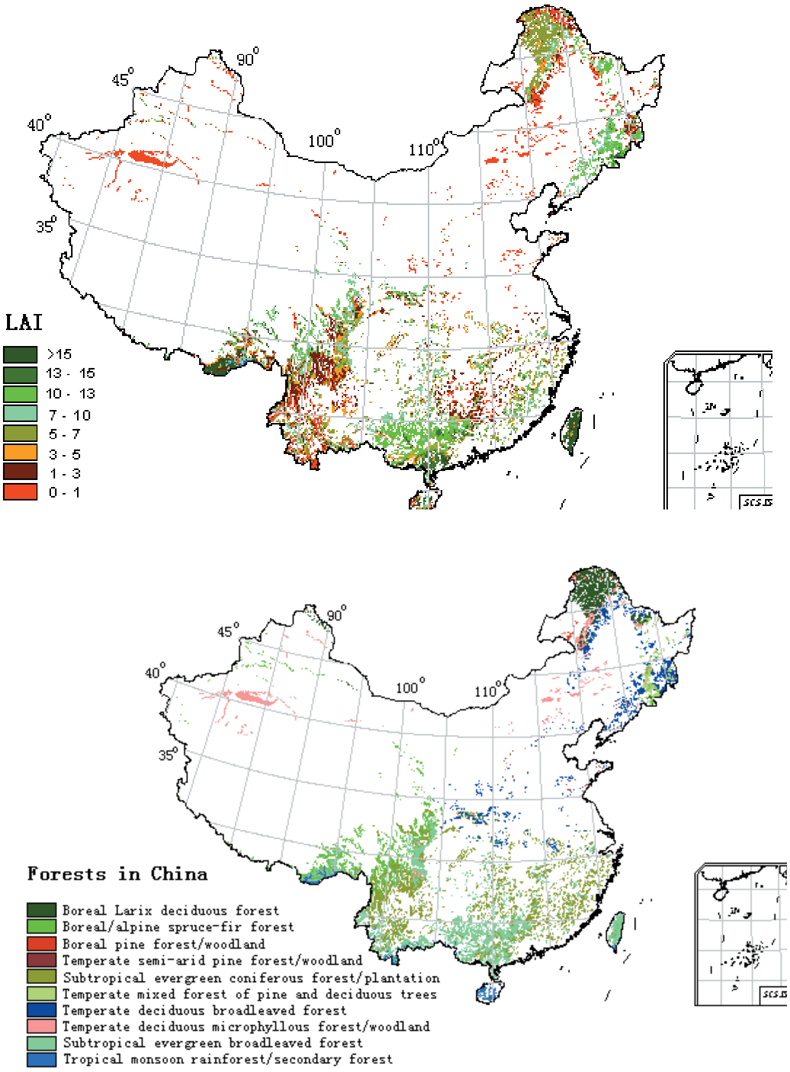

Fig. 7. Maximum *LAI* estimates (top) for forests in China (bottom) by the PhenLAI model.

of *LAI* measurements among different methods in three forest types in Dinghushan Reserve. The *LAI* of a 200-yr monsoon evergreen broad-leaved forest in the reserve was measured by four methods: 17.76 by empirical allometric regressions, 17.60 by inclined point quadrats, 16.99 from light interception, and 6.57 from litter fall. Here, the first three methods have the same estimates. According to the analysis of Ren & Peng (1997), the serious underestimate from litter fall is because of the influences of frequent typhoon and storm in the region. The measurements from the mixed forest of pine and broad-leaved trees and the pine pure forest in the reserve indicated similar differences among the four methods. We believe that forest *LAI* in China is commonly > 6, especially in tropical rainforest, subtropical evergreen broad-leaved forest, temperate mixed forest, and boreal/ alpine *Picea-Abies* forest (from Tables 3-5), although there is uncertainty in *LAI* measurements by different methods.

Generally, while stand *LAI* is > 6 or 7, forest growth efficiency decreases and total above-ground net primary productivity reaches a maximum and keeps constant (Waring & Schlesinger 1985). However, it is still unclear why some forest types, such as boreal/temperate *Picea-Abies* forest and tropical/subtropical evergreen broad-leaved forest, can keep such high *LAI* values of > 6 or 7, and what their biological function is. For *Picea-Abies* forests in the cold-temperate zone or on alpine mountains, long leaf life span and high canopy leaf mass have three advantages (Chapin 1980; Chabot & Hicks 1982): (1) maximizing the utilization of sunlight available and compensating for low rates of photosynthesis by large leaf area for light interception, (2) moderating the recycling of nutrients through litter fall and decomposition processes and increasing nutrient use efficiency, and (3) serving as storage organs for carbohydrates and mineral nutrients in avoiding problems with translocation through frozen soils to support early season growth. For

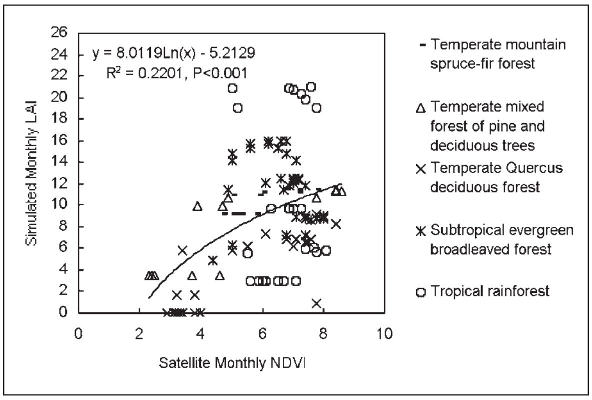

Fig. 8. Relationship between satellite monthly *NDVI* and simulated monthly *LAI* for the nine undisturbed forest sites in Table 4. The *LAI-NDVI* comparison clearly demonstrates the lack of a relation between *LAI* and *NDVI*, because of the saturation problem in satellite detection of high forest *LAI*.

tropical or subtropical evergreen broad-leaved forests, high canopy leaf mass would favour mineral conservation in avoiding problems with the leaching of nutrients from leaves and soil due to high rainfall and temperature (Monk 1966).

Limitations of the PhenLAI model

In closed-canopy forest stands, there is a significant relationship between foliage mass and leaf life span (Reich et al. 1992). Moreover, variations in leaf life span are a strategy for optimizing plant carbon gain (Kikuzawa 1991, 1995) and for plant adaptations to specific temperature, moisture and nutrient regimes (Monk 1966; Waring & Franklin 1979; Chapin 1980; Chabot & Hicks 1982; Reich et al. 1991). The PhenLAI model, however, lacked such a general process modelling of leaf life span where the minimum *LAI* was estimated by using a leaf-retention fraction based on the average leaf life span in different forest types that would filter different wavelengths of interannual weather variability.

The predictions of seasonal *LAI* patterns were generally consistent with the satellite *NDVI* changes in timing and dynamics, but we need direct measurements of seasonal stand *LAI* to validate the simulations of monthly *LAI* in future work. However, there remains a problem in the methodology for measuring seasonal *LAI* of forests. Little information about seasonal changes of *LAI* in forests, especially in evergreen forests, has been available.

We should note that the water balance model did not consider more detailed hydrological processes in forest ecosystems and the effect of underground water. The next step of this work needs to take into account the feedback of *LAI* growth and improve the parameters such as stomatal conductance, rooting depth, etc.

Future directions

The PhenLAI model suggests the possibility to develop an ecological approach to the high *LAI* problem in remote sensing and provide a helpful or convenient approach for calibrating the more sophisticated ecosystem models. A general process modelling of leaf life span would improve our ability to predict *LAI* of forests and to develop a regional dynamic vegetation model coupling biogeochemistry with phytogeography. Previous studies noted above suggested that the geographical distribution patterns of *LAI* would be controlled not only by soil water balance, but also by other physiological constraints such as the strategy for maximizing carbon gain, mineral conservation mechanisms and nutrient-use efficiency. Many theories have been proposed to explain or simulate the variations in leaf habit, leaf life span and their geographical patterns. Waring & Franklin (1979) suggested that the combined effects of plant adaptations to temperature, moisture and nutrient regimes favour the evolution of the massive, evergreen coniferous forests of the Pacific Northwest in contrast to the deciduous hardwood forests in other temperate regions. Ewers & Schmid (1981) indicated that there is a strong positive correlation between elevation and retention time of dwarf shoots (needle fascicle), based on field data for eight taxa (21 populations) of *Pinus* growing at various elevations in California and other data from literature for the 37 species of *Pinus* native to the United Stated and Canada

The PhenLAI model is not applicable to young forests because stand ages of forests are closely related to *LAI* growth, especially in secondary forests and plantations. Although it is possible to simulate *LAI* growth with stand age, it remains a problem how to obtain spatial information on stand age.

Acknowledgements: This study is funded by the National Key Projects for Basic Research of China (G1998040813, G2000046807), the Knowledge Innovation Project of Chinese Academy of Sciences (CX10G-C00-02, CX10G-E01-02-03), the International Cooperation Project of the USDA Forest Service Northern Global Change Program (Award No.: 00--CA-11242343-017), and the Outstanding Young Scientist Program of the National Natural Science Foundation of China (30125036). The model and a first manuscript were prepared in the Ecosystem Center of MBL, Woods Hole, USA when T. Luo stayed there under the Foreign Training Program of the Chinese Ecosystem Research Network (CERN) from a loan project of the World Bank. We thank Mrs. D.W. Kicklighter and J. Helfrich for help with programming, and Drs. J. M. Melillo, Y. Pan and X. Xiao for helpful comments.

References

Anon. (USGS EROS). *Global 1-km AVHRR-NDVI 10-day composite data (1995.2-1996.1)*. http://edcdaac. usgs.gov/1km/comp10d.html

Anderson, R.C. 1974. Seasonality in terrestrial primary producers. In: Lieth, H. ed. *Phenology and seasonality modeling*, pp. 103-112. Springer-Verlag, New York, NY.

Bormann, F.H. & Likens, G.E. 1979. *Patterns and process in a forested ecosystem.* Springer-Verlag, Berlin, DE.

Cannell, M.G.R. & Smith, R.I. 1983. Thermal time, chill days and prediction of budburst in *Picea sitchensis*. *J. Appl. Ecol.* 20: 951-963.

Chabot, B.F. & Hicks, D.J. 1982. The ecology of leaf life spans. *Annu. Rev. Ecol. Syst.* 13: 229-259.

Chapin, F.S. III. 1980. The mineral nutrition of wild plants. *Annu. Rev. Ecol. Syst.* 11: 233-260.

Chapin, F.S. III & Tryon, P.R. 1983. Habitat and leaf habit as determinant of growth, nutrient absorption, and nutrient use by Alaskan taiga forest species. *Can. J. For. Res.* 13: 818-826.

Cihlar, J., Denning, A.S. & Gosz, J. (eds.) 2000. *Global terrestrial carbon observation: requirements, present status, and next steps*. TCO Synthesis Workshop, 8-11 February, Ottawa, CA.

Curran, P.J., Dungan, J.L. & Gholz, H.L. 1992. Seasonal *LAI* in slash pine estimated with Landsat TM. *Remote Sens. Environ.* 39: 3-13.

Daly, C., Neilson, R.P. & Phillips, D.L. 1994. A statistical-topographic model for mapping climatological precipitation over mountainous terrain. *J. Appl. Meteorol.* 33: 140-158.

Daly, C., Taylor, G.H., Gibson, W.P., Parzybok, T.W., Johnson, G.L. & Pasteris, P.A. 2000. High-quality spatial climate data sets for the United States and beyond. *Trans. ASAE* 43: 1957-1962.

Daughtry, C.S.T., Gallo, K.P., Goward, S.N., Prince, S.D. & Kustas, W.P. 1992. Spectral estimates of absorbed radiation and phytomass production in corn and soybean canopies. *Remote Sens. Environ.* 39: 141-152.

Eamus, D. 1991. The interaction of rising CO_2 and temperature with water use efficiency. *Plant Cell Environ.* 14: 843-852.

Ewers, F.W. & Schmid, R. 1981. Longevity of needle fascicles of *Pinus longaeva* (Bristlecone pine) and other North American pines. *Oecologia* 51: 107-115.

Field, C. & Mooney, H.A. 1983. Leaf age and seasonal effects on light, water, and nitrogen use efficiency in a California shrub. *Oecologia* 56: 348-355.

Field, C.B., Randerson, J.T. & Malmstron, C.M. 1995. Global net primary production: combining ecology and remote sensing. *Remote Sens. Environ.* 51: 74-88.

Gill, D.S. & Mahall, B.E. 1986. Quantitative phenology and water relations of an evergreen and a deciduous chaparral shrub. *Ecol. Monogr.* 56: 127-143.

Goetz, S.J. & Prince, S.D. 1996. Remote sensing of net primary production in boreal forest stands. *Agricult. For. Meteorol.* 78: 149-179.

Grier, C.C. & Running, S.W. 1977. Leaf area of mature northwestern coniferous forests: relation to site water balance. *Ecology* 58: 893-899.

Hou, X.-Y. 1979. *Vegetation map of China* (1:4,000,000). China Atlas Press, Beijing, CN.

Hunt, E.R. Jr, Piper, S.C., Nemani, R., Keeling, C.D., Otto, R.D. & Running, S.W. 1996. Global net carbon exchange and intra-annual atmospheric CO_2 concentrations predicted by an ecosystem process model and three-dimensional atmospheric transport model. *Global Biogeochem. Cycl.* 10: 431-456.

Hunter, A.F. & Lechowicz, M.J. 1992. Predicting the timing of budburst in temperate trees. *J. Appl. Ecol.* 29: 597-604.

Janecek, A., Benderoth, G., Lüdeke, M.K.B., Kindermann, J., Kohlmaier, G.H. 1989. Model of the seasonal and perennial carbon dynamics in deciduous-type forests controlled by climatic variables. *Ecol. Model.* 49: 101-124.

Kikuzawa, K. 1983. Leaf survival of woody plants in deciduous broadleaved forests. 1. Tall trees. *Can. J. Bot.* 61: 2133- 2139.

Kikuzawa, K. 1984. Leaf survival of woody plants in deciduous broadleaved forests. 2. Small trees and shrubs. *Can. J. Bot.* 62: 2551-2556.

Kikuzawa, K. 1991. A cost-benefit analysis of leaf habit and leaf longevity of trees and their geographical pattern. *Am. Nat.* 138: 1250-1263.

Kikuzawa, K. 1995. Leaf phenology as an optimal strategy for carbon gain in plants. *Can. J. Bot.* 73: 158-163.

Kunkel, K.E. 1990. Operational soil moisture estimation for the midwestern United States. *J. Appl. Meteorol.* 29: 1158-1166.

Landsberg, J.J. 1974. Apple fruit bud development and growth: analysis and an empirical model. *Ann. Bot.* 38: 1013-1023.

Larcher, W. 1975. *Physiological plant ecology*. Springer-Verlag, New York, NY.

Li, C-H., Fukushima, Y. & Suzuki, M. 2001. The waterflow property of the small watersheds covered with evergreen broadleaved forest in Jiulian Mountain. *Resour. Sci.* 23 (Suppl.): 36-57. (In Chinese.)

Lieth, H. 1970. Phenology in productivity studies. In: Reichle, D.E. (ed.) *Analysis of temperate forest ecosystems*, pp. 29-46. Springer, New York, NY.

Liu, S.-R., Wen, Y.-G., Wang, B. & Zhou, G.-Y. 1996. *Ecohydrological functions of forest ecosystems in China*. China Forestry Publishing House, Beijing. (In Chinese.)

Liu, Y-C., Wu, M-Z., Guo, Z-M., Jiang, Y-X., Liu, S-R., Wang, Z-Y., Liu, B-D. & Zhu, X-L. 1998. Biomass and net productivity of *Quercus variabilis* forest in Baotianman Natural Reserve. *Chin. J. Appl. Ecol.* 9: 569-574. (In Chinese.)

Lowman, M.D. 1992. Leaf growth dynamics and herbivory in five species of Australian rain-forest canopy trees. *J. Ecol.* 80: 433-447.

Luo, T.-X. 1996. *Patterns of net primary productivity for Chinese major forest types and their mathematical models*. Ph.D. Dissertation, Chinese Academy of Sciences, Beijing, CN.

Luo, T.-X., Li, W.-H. & Zhao, S.-D. 1997. Distribution patterns of leaf area index for major coniferous forest types in China. *J. Chin. Geogr.* 7: 61-73.

Marshall, J.D. & Waring, R.H. 1986. Comparison of methods of estimating leaf-area index in old-growth Douglas-fir. *Ecology* 67: 975-979.

McMurtrie, R. & Wolf, L. 1983. A model of competition between trees and grass for radiation, water and nutrients. *Ann. Bot.* 52: 449-458.

Monk, C.D. 1966. An ecological significance of evergreenness. *Ecology* 47: 504-505.

Murray, M.B., Cannell, M.G.R. & Smith, R.I. 1989. Date of budburst of fifteen tree species in Britain following climate warming. *J. Appl. Ecol.* 26: 693-700.

Neilson, R.P. 1995. A model for predicting continental-scale vegetation distribution and water balance. *Ecol. Appl.* 5: 362-385.

New, M., Hulme, M. & Jones, P.D. 2000. *Global 30-year mean monthly climatology, 1961-1990*. http://www.daac.ornl. gov/

Odum, E.P. 1971. *Fundamentals of ecology* (3th ed.). Saunders, London, UK.

Prentice, I.C., Cramer, W., Harrison, S.P., Leemans, R., Monserud, R.A. & Solomon, A.M. 1992. A global biome model based on plant physiology and dominance, soil properties and climate. *J. Biogeogr.* 19: 117-134.

Prince, S.D. 1991a. Satellite remote sensing of primary production: comparison of results for Sahelian grasslands 1981-1988. *Int. J. Remote Sens.* 12: 1301-1311.

Prince, S.D. 1991b. A model of regional primary production for use with coarse resolution satellite data. *Int. J. Remote Sens.* 12: 1313-1330.

Reich, P.B., Uhl, C., Walters, M.B. & Ellsworth, D.S. 1991. Leaf life span as a determinant of leaf structure and function among 23 Amazonian tree species. *Oecologia* 86: 16-24.

Reich, P.B., Walters, M.B. & Ellsworth, D.S. 1992. Leaf life span in relation to leaf, plant, and stand characteristics among diverse ecosystems. *Ecol. Monogr.* 62: 365-392.

Ren, H. & Peng, S.-L. 1997. Comparison of methods for estimating leaf area index in Dinghushan forests. *Acta Ecol. Sin.* 17: 220-223. (In Chinese.)

Ruimy, A., Saugier, B. & Dedieu, G. 1994. Methodology for the estimation of terrestrial net primary productivity from remotely sensed data. *J. Geophys. Res.* 99: 5263-5283.

Running, S.W., Nemani, R.R., Peterson, D.L., Band, L.E, Potts, D.F., Pierce, L.L. & Spanner, M.A. 1989. Mapping regional forest evapotranspiration and photosynthesis by coupling satellite data with ecosystem simulation. *Ecology* 70: 1090-1101.

Saugier, B. & Katerji, N. 1991. Some plant factors controlling evapotranspiration. *Agric. For. Meteorol.* 54: 263-277.

Saxton, K.E., Rawls, W.J., Romberger, J.S. & Papendick, R.I. 1986. Estimating generalized soil-water characteristics from texture. *Soil Sci. Soc. Am. J.* 50: 1031-1037.

Scurlock, J.M.O., Asner, G.P. & Gower, S.T. 2001. *Global leaf area index from field measurements, 1932-2000*. http://www.daac.ornl.gov/

Sellers, P.J. 1985. Canopy reflectance, photosynthesis, and transpiration. *Int. J. Remote Sensing* 6: 1335-1372.

Sharik, T.L. & Barnes, B.V. 1976. Phenology of shoot growth among diverse populations of yellow birch (*Betula allegheniensis*) and aweet birch (*B. lenta*). *J. Bot.* 54: 2122-2129.

Spanner, M.A., Pierce, L.L., Running, S.W. & Peterson, D.L. 1990. The seasonality of AVHRR data of temperate coniferous forests: relationship with leaf area index. *Remote Sens. Environ.* 33: 97-112.

Stephenson, N.L. 1990. Climatic control of vegetation distribution: the role of the water balance. *Am. Nat.* 135: 649-670.

Tadaki, Y. 1977. Leaf biomass. In: Shidei, T. & Kira, T. (eds.) *Primary productivity of Japanese forests: productivity of terrestrial communities*. JIBP Synthesis 16: 39-44. University of Tokyo Press, Tokyo, JP.

Taylor, F.G. Jr. 1974. Phenodynamics of production in a mesic deciduous forest. In: Lieth, H. (ed.) *Phenology and seasonality modeling*, pp. 237-254. Springer, New York, NY.

Thomson, A.J. & Moncrieff, S.M. 1982. Prediction of bud burst in Douglas-fir by degree-day accumulation. *Can. J. For. Res.* 12: 448-452.

Thornthwaite, C.W. & Mather, J.R. 1957. Instructions and tables for computing potential evapotranspiration and the water balance. *Public. Climatol.* 10: 183-311. University of Delaware, US.

Tian, H., Hall, C.A.S. & Qi, Y. 1998. Modeling primary productivity of the terrestrial biosphere in changing environments: toward a dynamic biosphere model. *Crit. Rev. Plant Sci.* 15: 541-557.

Tsutsumi, T., Li, C.-H., Iwatsubo, G., Li, W.-H., Tamai, S., Chiba, K. & Katagiri, S. 2001. A study on the evergreen broadleaved forest in the Jiulian Mountain of Jiangxi Province. *Resources Sci.* 23: 15-35. (In Chinese.)

Vörösmarty, C.J., Moore, B. III, Grace, A.L., Gildea, M.P., Melillo, J.M., Peterson, B.J., Rastetter, E.B. & Steudler, P.A. 1989. Continental scale models of water balance and fluvial transport: an application to South America. *Glob. Biogeochem. Cycl.* 3: 241-265.

Waggoner, P.E. 1974. Modeling seasonality. In: Lieth, H. (ed.) *Phenology and seasonality modeling*, pp. 301-322. Springer-Verlag, New York, NY.

Wang, J. 1960. A critique of the heat unit approach to plant response studies. *Ecology* 41: 785-790.

Waring, R.H. & Franklin, J.F. 1979. Evergreen coniferous forests of the Pacific Northwest. *Science* 204: 1380-1386.

Waring, R.H. & Schlesinger, W.H. 1985. *Forest ecosystems: concepts and management*. Academic Press, Inc., Orlando, FL.

Webb, R.W., Rosenzweig, C.E. & Levine, E.R. 2000. Global soil texture and derived water-holding capacities. http://www.daac.ornl.gov/

Webb, W.L., Lauenroth, W.K., Szarek, S.R., Kinerson, R.S. 1983. Primary production and abiotic controls in forests, grasslands, and desert ecosystems in the United States. *Ecology* 64: 134-151.

White, M.A., Thornton, P.E. & Running, S.W. 1997. A continental phenology model for monitoring vegetation responses to interannual climatic variability. *Global Biogeochem. Cycl.* 11: 217-234.

Woodward, F.I. 1987. *Climate and plant distribution*. Cambridge University Press, Cambridge, UK.

Woodward, F.I., Smith, T.M. & Emanuel, W.R. 1995. A global primary productivity and phyto-geography model. *Glob. Biogeochem. Cycl.* 9: 471-490.

Xie, S.-C., Sheng, C.-Y. & Li, S.-C. 1997. A phenological study on main tree species of montane humid evergreen broadleaved forest in Ailao Mountains. *Acta Ecol. Sin.*17(1): 51-60. (In Chinese.)

Received 22 March 2002
Revision received 22 August 2002
Accepted 22 August 2002
Coordinating Editor: C. Leuschner

For App. 1-4, see JVS/AVS Electronic Archives; www.opuluspress.se/pub/archives/index.htm